Enhanced backstepping control for disturbances rejection in quadrotors

Ali Saibi[1], Hadjira Belaidi[1], Razika Boushaki[2], Recham Zine Eddine[3], Amrouche Hafid[3]
[1]Signal and Systems Laboratory, Institute of Electrical and Electronic Engineering, University M'hamed Bougara of Boumerdes, Boumerdes, Algeria
[2]Laboratoire d'Automatique Appliquée, Institute of Electrical and Electronic Engineering, University M'hamed Bougara of Boumerdes, Boumerdes, Algeria
[3]Institute of Electrical and Electronic Engineering, University M'hamed Bougara of Boumerdes, Boumerdes, Algeria

Article Info

ABSTRACT

This work studies the issue of quadrotor trajectory tracking control in presence of disturbances and model uncertainties. The paper starts by extracting the kinematics and dynamics models of the quadrotor. This results in the motion equations, which eventually serve as a blueprint for creating the suggested smart flight control scheme. Secondly, an enhanced backstepping controller (BSC) is developed and tested to keep the quadrotor tracking the desired trajectory both in steady state and in presence of disturbances. Finally, BSC beside two other controllers: sliding mode controller (SMC) and proportional derivative controller (PDC) are implemented in MATLAB/Simulink and the obtained results are compared and conclusions are extracted. Therefore, it is established that PDC is not robust to disturbances as noise will be amplified due to the derivative term. Whereas, although SMC is robust to parameter variations and disturbances; however, it is not continuous which may affect the actuators due to the increased gains which may saturate them. In contrast, BSC requires too many tuning parameters; however, it ensures Lyapunov Stability and does not depend on the system as it does not involve cancelling system nonlinearity. Moreover, BSC results are 10^{17} better than the results of the two other controllers.

Corresponding Author:

Ali Saibi
Signals and Systems Laboratory Institute of Electrical and Electronic Engineering
University M'hamed Bougara of Boumerdes
35000 Boumerdes, Algeria
Email: a.saibi@univ-boumerdes.dz

1. INTRODUCTION

Unmanned aerial vehicles drones (known as UAVs) are self-flying robots. In several circumstances, it is preferable that the system achieves significant movements, moves both vertically and horizontally, and be as tiny as feasible. With the advancement of UAVs' technology, their applications are extended to surveillance, healthcare, agriculture, civil and military fields, transmission line inspection and energy delivery [1]–[3]. Drones provide a number of fundamental advantages over conventional aircraft systems, including increased flexibility, reduced price, fewer radar scans, a longer lifespan, and no harm to the operator's life. The quadrotor rolls and pitches in the direction of the slowly rotating motor. By dividing the thrust into two directions, represented by the roll and pitch angles, linear motion is generated. However, actually, the drone is considered a nonlinear system with resilient coupling and under-actuated characteristics [4], [5]. It can also be significantly impacted by outside disturbances like wind gusts. Therefore, the quadrotor provides a hard control problem

because of its very unsteady characteristics [6]. Hence, the need for an effective control method arises from the peculiar nature of the aerial vehicle.

Recently, proportional integral derivative (PID) controller based on optimization algorithms [7]–[9] and fuzzy logic [10]–[13] have proved their efficiency in terms of controlling such nonlinear, unstable systems; however, their implementation on quadrotors was very limited because of the presence of external disturbances which are hard to be predicted. In the literature, several techniques were developed for vehicles' control in general [14]–[16] and for quadrotors' control in particular such as sliding mode controller (SMC) [17], SMC approach built on backstepping controller (BSC) which produces high performances and faster response [18], [19], sliding controller combined with state observer compensate for uncertain nonlinear components [20]. As well, Backstepping based nonlinear control and adaptive SMC [21], PID control [22]–[25], nonlinear adaptive and predictive controllers [26]–[28], plus the controller eliminating active disturbances (ADRC) which deals with the study of path following performances where considering outer factors [4]. Besides, adaptive proportional integral derivative (APID) controllers ensured faster convergence speed and minimum overshoot in the existence of constraint variations and outside instabilities [29], [30].

The BSC has proved its efficacy in the control of nonlinear systems compared to the other controllers, especially with the influence of exterior forces [5], [31]. Research by Fahmizal *et al.* [32] the three approaches (PID, SMC, and BSC) were applied to a standalone photovoltaic system's single-phase voltage inverter; the authors proved that BSC has the potential to perform better than the other two controllers. Hence, our work explores the issue of quadrotor trajectory tracking control with the influence of disturbances and model uncertainties. First, the kinematics and dynamics of the quadrotor are described in detail to aid in understanding the behavior of the drone. The motion equations that result from this [33] are then employed as a blueprint for creating the suggested smart flight control strategy. In this work, an easy-to-implement enhanced BSC is developed; then, tested beside two other controllers: sliding mode (BSC) and proportional derivative controller (PDC) to keep the quadrotor tracking the desired trajectory both in steady state and in the existence of outside instabilities. Finally, the three controllers' results are compared to determine which is the best.

2.   METHOD

The distance between the body and the earth frames $r = [x\ y\ z]^T$ reveals the precise location of the quadrotor's center of mass. The roll (ϕ), pitch (θ), and yaw (ψ) angles, which denote rotations about the X, Y, and Z axes, respectively, characterize the orientation of the quadrotor. The orientation of the quadrotor is expressed by the rotation R from the inertial to the body frame. Supposing that the rotation occurs in the following order: pitch, roll, and yaw; thus, R is assumed by (1) [34], [35]:

$$R = \begin{bmatrix} cos(\theta)\,cos\,(\psi) & cos(\psi)\,sin(\theta)\,sin(\phi) - cos(\phi)\,sin\,(\psi) & cos(\phi)\,sin(\theta)\,cos(\psi) + sin(\phi)\,sin\,(\psi) \\ cos(\theta)\,sin\,(\psi) & sin(\phi)\,sin(\theta)\,sin(\psi) + cos(\theta)\,cos\,(\psi) & cos(\phi)\,sin(\theta)\,sin(\psi) - sin(\theta)\,cos\,(\psi) \\ -sin\,(\theta) & sin(\phi)\,cos\,(\theta) & cos(\phi)\,cos\,(\theta) \end{bmatrix} \quad (1)$$

in order to connect the inertial frame-measured Euler rates $\dot{\eta} = [\dot{\phi}\ \ \dot{\theta}\ \ \dot{\psi}]^T$ and the rates of the angular body $\omega = [p\ \ q\ \ r]^T$, the following conversion is required [34]: $\omega = R_r\dot{\eta}$. With:

$$R_r = \begin{bmatrix} cos(\theta) & 0 & -cos(\phi)\,sin(\theta) \\ 0 & 1 & sin(\phi) \\ sin(\theta) & 0 & cos(\phi)\,cos(\theta) \end{bmatrix} \quad (2)$$

small angle assumptions are made around the hover location where $cos(\phi) \approx cos(\theta) \approx 1$ and $sin(\phi) \approx sin(\theta) \approx 0$. R_r can therefore be reduced to an identity matrix I [36].

2.1. Quadrotor dynamics

Quadrotor's movement may be split into 2 control systems: a rotating sub-system (roll, pitch, and yaw) and a translating sub-system (x, y, and z coordinates). The revolving sub-system is completely actuated whilst translating sub-system is under-actuated [37]. Newton Euler equation can be formulated by (3):

$$\begin{bmatrix} F \\ \tau \end{bmatrix} = \begin{bmatrix} mI_{d3} & O_3 \\ O_3 & I_3 \end{bmatrix} \begin{bmatrix} a \\ \alpha \end{bmatrix} + \begin{bmatrix} 0 \\ \omega \times I_3\omega \end{bmatrix} \qquad I_3 = \begin{bmatrix} I_{xx} & 0 & 0 \\ 0 & I_{yy} & 0 \\ 0 & 0 & I_{zz} \end{bmatrix} \quad (3)$$

With: F: net force acting on the quadrotor
         τ: net torque

I_{d3}: 3×3 identity matrix
I_3: moment of inertia
m: the mass of the quadrotor
a: the center of mass's linear acceleration
α: angular acceleration

2.1.1. Rotational subsystem

In the body frame, based on the Newton-Euler method the rotational equations of motion are derived using the general formalism (4):

$$I\dot{\omega} + \omega \times I\omega = M_B \tag{4}$$

Where: I: is the inertia matrix of the quadrotor
ω: is the angular body rate
M_B: are all the moments acting on the quadrotor in the body frame
$I\dot{\omega} \ and \ \omega \times I\omega$: represent the rate of change of angular momentum in the body frame

2.1.2. Matrix of inertia

The quadrotor's inertia matrix is a diagonal matrix, and because of the symmetry of the quadrotor, the off-diagonal elements, which make up the inertia product, are zero as shown in (3). Ixx, Iyy, and Izz are the body frame's primary axes' respective area moments of inertia. Before defining the last term (M_B) of (4), two physical effects have to be defined: the rotor-generated moments and aerodynamic forces. Each rotor produces a force called the aerodynamic force F_i and a moment called the aerodynamic moment M_i as a result of rotation [32]. They are given by (5) and (6):

$$F_i = \frac{1}{2}\rho A C_T r^2 \Omega_i^2 = K_f \Omega_i^2 \tag{5}$$

$$M_i = \frac{1}{2}\rho A C_D r^2 \Omega_i^2 = K_M \Omega_i^2 \tag{6}$$

Where: ρ: is the air density
A: blade area
C_D, C_T: aerodynamic coefficients
r: radius of blade
Ω_i: angular velocity of rotor i
K_f, K_M: are the aerodynamic force and moment constants respectively.
Figure 1 depicts the forces and moments acting on each of the quadrotor's four rotors.
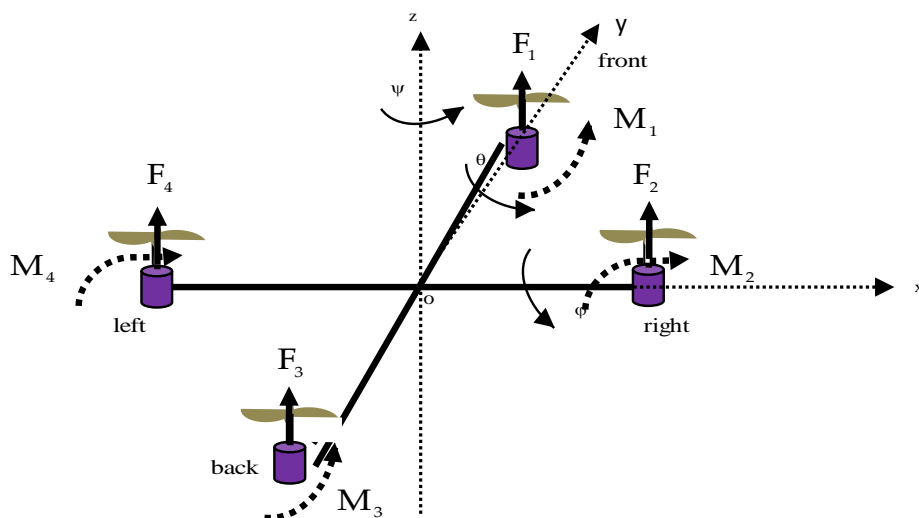

Figure 1. Moments and forces affecting the quadrotor's motion

It is obvious that each rotor creates a moment M_i with a direction opposite to the corresponding rotor's directions and an upward thrust force F_i. By relating the moments around the axes of the body, the right-hand rule combined with the body frame's axes facilitate the deriving of the equations of M_B [35], which are written:

$$M_B = \begin{bmatrix} lK_f(-\Omega_2^2 + \Omega_4^2) \\ lK_f(\Omega_1^2 - \Omega_3^2) \\ K_M(-\Omega_1^2 + \Omega_2^2 - \Omega_3^2 + \Omega_4^2) \end{bmatrix} \tag{7}$$

so, by replacing M_B in (4) and from (1) we can get:

$$\begin{bmatrix} \dot{\phi} \\ \dot{\theta} \\ \dot{\psi} \end{bmatrix} = \begin{bmatrix} cos(\theta) & 0 & sin(\theta) \\ sin(\theta)\,tan(\phi) & 1 & -cos(\theta)\,tan(\phi) \\ -\frac{sin(\theta)}{cos(\phi)} & 0 & \frac{cos(\theta)}{cos(\phi)} \end{bmatrix} \begin{bmatrix} p \\ q \\ r \end{bmatrix} \tag{8}$$

2.1.3. Motion's translational equations

Using the Earth's frame and Newton's second rule of motion, the linear equations of motion are given by:

$$m\ddot{r} = \begin{bmatrix} 0 \\ 0 \\ -mg \end{bmatrix} - F_a + RF_B \tag{9}$$

Where: $r = [x \quad y \quad z]^T$ define the distance of the quadrotor from the inertial frame
g: acceleration due to gravity $g = 9.81 \; m/s^2$
F_a: drag forces
F_B: nongravitational forces. To translate the thrust forces from the body frame into the inertial frame, non-gravitational forces operating on the quadrotor are multiplied by the rotation matrix
The nongravitational forces F_B, the resisting force F_a and the drag moment M_a could be stated as:

$$F_B = \begin{bmatrix} 0 \\ 0 \\ K_f(\Omega_1^2 + \Omega_2^2 + \Omega_3^2 + \Omega_4^2) \end{bmatrix} \tag{10}$$

$$F_a = K_t \dot{r} \tag{11}$$

$$M_a = K_r \dot{\eta} \tag{12}$$

Where: K_t: a constant matrix called the aerodynamic translation coefficient matrix
$\dot{r}$: the derivative of the position vector r (velocity of the quadrotor)
K_r: a constant matrix called the aerodynamic rotation coefficient matrix
$\dot{\eta}$: the Euler rate
From (4) can be written as:

$$I\dot{\omega} + \omega \times I\omega + M_G = M_B - M_a \tag{13}$$

2.2. State space representation

Due to a lack of sensors, state variable measuring is expensive and challenging in reality [38], [39]. Thus, quadrotor's state vector is defined as:

$$X = [x_1\ x_2\ x_3\ x_4\ x_5\ x_6\ x_7\ x_8\ x_9\ x_{10}\ x_{11}\ x_{12}]^T \tag{14}$$

this is translated into the degrees of freedom of the quadrotor presented in (2). The quadrotor's position in space, together with its angular and linear velocities, are all indicated by the state vector as:

$$X = \begin{bmatrix} \phi\ \dot{\phi}\ \theta\ \dot{\theta}\ \psi\ \dot{\psi}\ z\ \dot{z}\ x\ \dot{x}\ y\ \dot{y} \end{bmatrix}^T \tag{15}$$

having: $U_1 = K_f(\Omega_1^2 + \Omega_2^2 + \Omega_3^2 + \Omega_4^2), U_2 = K_f(-\Omega_2^2 + \Omega_4^2), U_3 = K_f(\Omega_1^2 - \Omega_3^2),$

$$U_4 = K_M(-\Omega_1^2 + \Omega_2^2 - \Omega_3^2 + \Omega_4^2)$$

$$a_1 = \frac{I_{yy} - I_{zz}}{I_{xx}}, a_2 = \frac{I_{zz} - I_{xx}}{I_{yy}}, a_3 = \frac{I_{xx} - I_{yy}}{I_{zz}}, b_1 = \frac{l}{I_{xx}}, b_2 = \frac{l}{I_{yy}}, b_3 = \frac{l}{I_{zz}}$$

$$\dot{x}_1 = \dot{\phi} = x_2$$
$$\dot{x}_2 = \ddot{\phi} = a_1 x_4 x_6 - a_2 x_4 \Omega + b_1 U_2$$
$$\dot{x}_3 = \dot{\theta} = x_4$$
$$\dot{x}_4 = \ddot{\theta} = x_2 x_6 a_3 + a_4 x_2 \Omega + b_2 U_3$$
$$\dot{x}_5 = \dot{\psi} = x_6$$
$$\dot{x}_6 = \ddot{\psi} = x_2 x_4 a_5 + b_3 U_4$$
$$\dot{x}_7 = \dot{z} = x_8 \tag{16}$$
$$\dot{x}_8 = \ddot{z} = -g + \frac{U_1}{m} cos(x_1) cos(x_2)$$
$$\dot{x}_9 = \dot{x} = x_{10}$$
$$\dot{x}_{10} = \ddot{x} = \frac{U_1}{m}(sin\, x_1\, sin\, x_5 + cos\, x_1\, sin\, x_3\, cos\, x_5)$$
$$\dot{x}_{11} = \dot{y} = x_{12}$$
$$\dot{x}_{12} = \ddot{y} = \frac{U_1}{m}(-sin\, x_1\, cos\, x_5 + cos\, x_1\, sin\, x_3\, sin\, x_5)$$

2.3. Quadrotor's backstepping control

Backstepping control is a recursive Lyapunov based control technique for systems in strict feedback form, it works by cascading a number of sub-systems into the main system. The control rules are then developed, one for the entire system and one for each subsystem, in decreasing order. The elaborated rules are given in the following sections.

2.3.1. Roll control

Taking into account the first stated sub-system:

$$\begin{cases} \dot{x}_1 = x_2 \\ \dot{x}_2 = a_1 x_4 x_6 - a_2 x_4 \Omega + b_1 U_2 \end{cases} \tag{17}$$

Step 1

The following is an expression for the error ε_1 between the desired and actual roll angles:

$$\varepsilon_1 = x_1^d - x_1 \tag{18}$$

Consider the Lyapunov function

$$V_1 = \frac{1}{2}\varepsilon_1^2$$

Therefore, V_1 is derived through x_1 variable, $\dot{V}_1$ is calculated as follow:

$$\dot{V}_1 = \varepsilon_1 \dot{\varepsilon}_1$$

With:

$$\dot{\varepsilon}_1 = \dot{x}_1^d - \dot{x}_1 = \dot{x}_1^d - x_2$$

Choosing

$$\dot{\varepsilon}_1 = -K_1 \varepsilon_1$$

(where: $K_1 \varepsilon_1$ positive definite function), we get:

$$x_2^d = \dot{x}_1^d + K_1 \varepsilon_1$$

Step 2

Denoting ε_2 the error among the actual roll angle rate and the desired one, thus:

$$\varepsilon_2 = x_2^d - x_2$$

Defining:

$$V_2 = V_1 + \frac{1}{2}\varepsilon_2^2$$

being a potential Lyapunov function

$$\dot{V}_2 = \dot{V}_1 + \varepsilon_2\dot{\varepsilon}_2 = \varepsilon_1\dot{\varepsilon}_1 + \varepsilon_2\dot{\varepsilon}_2 = -K_1\varepsilon_1^2 + \varepsilon_2(\varepsilon_1 + \dot{x}_2^d - x_4 x_6 a_1 + x_4\Omega a_2 - b_1 U)$$

Supposing

$$\varepsilon_2(\varepsilon_1 + \dot{x}_2^d - x_4 x_6 a_1 + x_4\Omega a_2 - b_1 U) = \text{-}K_2\varepsilon_2^2$$

$$U_2 = \frac{1}{b_1}(k_2\varepsilon_2 + \varepsilon_1 - x_4 x_6 a_1 + a_2 x_4\Omega - k_1 x_2) \tag{19}$$

2.3.2. Pitch control θ

Taking into account the second stated sub-system:

$$\begin{cases} \dot{x}_3 = x_4 \\ \dot{x}_4 = x_2 x_6 a_3 + a_4 x_2\Omega + b_2 U_3 \end{cases} \tag{20}$$

Step 1

Considering ε_3 the error among actual pitch angle rate and desired one and which can be obtained via:

$$\varepsilon_3 = x_3^d - x_3 \Rightarrow \dot{\varepsilon}_3 = \dot{x}_3^d - \dot{x}_3$$

Utilizing Lyapunov stability, pick:

$$V(\varepsilon_3) = \frac{1}{2}\varepsilon_3^2$$

The system trajectory is ensured to check the following condition if $\dot{V}$ is negative:

$$\dot{V}_3 = \varepsilon_3\dot{\varepsilon}_3 = \varepsilon_3(\dot{x}_3^d - x_4) < 0$$

Then:

$$\dot{x}_3^d - x_4 = -K_3\varepsilon_3 \Rightarrow \Rightarrow \quad x_4^d = \dot{x}_3^d + K_3\varepsilon_3$$

Step 2

The error:

$$\varepsilon_4 = x_4^d - x_4 \Rightarrow x_4 = x_4^d - \varepsilon_4$$

$$V_4 = V_3 + \frac{1}{2}\varepsilon_4^2 \rightarrow \quad \dot{V}_4 = \varepsilon_3\dot{\varepsilon}_3 + \varepsilon_4\dot{\varepsilon}_4 = \varepsilon_3(\dot{x}_3^d - x_4^d + \varepsilon_4) + \varepsilon_4(\dot{\varepsilon}_4)$$

Putting:

$$\varepsilon_4(\varepsilon_3 - x_2 x_6 a_3 - a_4 x_2\Omega + b_2 U_3) = -k_4\varepsilon_4^2$$

$$U_3 = \frac{1}{b_2}(-k_4\varepsilon_4 - \varepsilon_3 + x_2 x_6 a_3 + a_4 x_2\Omega + k_3 x_4) \tag{21}$$

2.3.3. Yaw angle control ψ

Now think about the third subsystem listed beneath:

$$\begin{cases} \dot{x}_5 = x_6 \\ \dot{x}_6 = x_2 x_4 a_5 + b_3 U_4 \end{cases} \tag{22}$$

Step 1

ε_5 describes the error among the actual yaw angle rate and the desired one. Accordingly:

$$\varepsilon_5 = x_5^d - x_5 \Rightarrow \dot{\varepsilon}_5 = \dot{x}_5^d - \dot{x}_5 -$$

with, Lyapunov function is

$$V(\varepsilon_5) = \frac{1}{2}\varepsilon_5^2 \Rightarrow \Rightarrow \quad \dot{V}_5 = \varepsilon_5 \dot{\varepsilon}_5$$

thus;

$$\dot{x}_5^d - \dot{x}_5 = -K_5 \varepsilon_5 \Rightarrow x_6^d = \dot{x}_5^d + K_5 \varepsilon_5$$

Step 2

The error

$$\varepsilon_6 = x_6^d - x_6 \Rightarrow x_6 = x_6^d - \varepsilon_6$$

$$V_6 = V_5 + \frac{1}{2}\varepsilon_6^2 \Rightarrow \dot{V}_6 = \varepsilon_5 \dot{\varepsilon}_5 + \varepsilon_6 \dot{\varepsilon}_6 \Rightarrow \dot{V}_6 = \varepsilon_5(\dot{x}_5^d - x_6^d + \varepsilon_6) + \varepsilon_6(\dot{\varepsilon}_6)$$

Naming:

$$\varepsilon_6(\varepsilon_5 - x_2 x_4 a_5 - \mathrm{k}_5 x_6 - \mathrm{b}_3 U_4) = -k_6 \varepsilon_6^2$$

$$U_4 = \frac{1}{b_3}(k_6 \varepsilon_6 + \varepsilon_5 - x_2 x_4 a_5 - k_5 x_6) \tag{23}$$

2.3.4. Altitude control

In (24) represents the fourth subsystem:

$$\begin{cases} \dot{x}_7 = x_8 \\ \dot{x}_8 = \frac{cos(x_1) \, cos(x_2)}{m} U_1 - g \end{cases} \tag{24}$$

Step 1

ε_7 describes the diference amongst the actual position z and desired one:

$$\varepsilon_7 = x_7^d - x_7 \Rightarrow \Rightarrow \quad \dot{\varepsilon}_7 = \dot{x}_7^d - \dot{x}_7 -$$

Lyapunov function is

$$V(\varepsilon_7) = \frac{1}{2}\varepsilon_7^2 \Rightarrow \Rightarrow \quad \dot{V}_7 = \varepsilon_7 \dot{\varepsilon}_7.$$

Then,

$$\dot{x}_7^d - x_8 = -K_7 \varepsilon_7 \Rightarrow \Rightarrow \quad x_8^d = \dot{x}_7^d + K_7 \varepsilon_7$$

Step 2

The error

$$\varepsilon_8 = x_8^d - x_8 \Rightarrow x_8 = x_8^d - \varepsilon_8 \Rightarrow \dot{\varepsilon}_8 = \dot{x}_8^d - \dot{x}_8.$$

Thus,

$$V_8 = V_7 + \frac{1}{2}\varepsilon_8^2 \Rightarrow \dot{V}_8 = \varepsilon_7\dot{\varepsilon}_7 + \varepsilon_8\dot{\varepsilon}_8$$

$$\varepsilon_7\dot{\varepsilon}_7 = \varepsilon_7(\dot{x}_7^d - x_8^d) + \varepsilon_7\varepsilon_8 + \varepsilon_8(\dot{\varepsilon}_8) = \varepsilon_8\left(\varepsilon_7 + \dot{x}_8^d - \left(g - \frac{U_1}{m}\cos(x_1)\cos(x_3)\right)\right)$$

Putting:

$$\varepsilon_8\left(\varepsilon_7 - \dot{x}_8^d - \left(g - \frac{U_1}{m}\cos(x_1)\,co\,s(x_2)\right)\right) = -k_8\varepsilon_8^2$$

Thus:

$$U_1 = \frac{m}{cos(x_1)cos\,(x_2)}(-\varepsilon_7 + g - k_8\,\varepsilon_{8\_}k_7x_7) \tag{25}$$

2.3.5. Control y position
Formula (26) denotes the fifth sub-system:

$$\begin{cases} \dot{x}_9 = x_{10} \\ \dot{x}_{10} = U_y\frac{U_1}{m} \end{cases} \tag{26}$$

Step 1

Defining ε_9 the difference concerning the actual position *y* and desired one:

$$\varepsilon_9 = x_9^d - x_9 \Rightarrow \dot{\varepsilon}_9 = \dot{x}_9^d - \dot{x}_9$$

The Lyapunov function is

$$V(\varepsilon_9) = \frac{1}{2}\varepsilon_9^2 \Rightarrow \dot{V}_9 = \varepsilon_9\dot{\varepsilon}_9$$

Then,

$$\dot{x}_9^d - x_{10} = -K_9\varepsilon_9 \Rightarrow \Rightarrow \quad x_{10}^d = \dot{x}_9^d + K_9\varepsilon_9$$

Step 2

Then, the error is:

$$\varepsilon_{10} = x_{10}^d - x_{10} \Rightarrow \dot{\varepsilon}_{10} = \dot{x}_{10}^d - \dot{x}_{10}$$

$$V_{10} = V_9 + \frac{1}{2}\varepsilon_{10}^2 \Rightarrow \dot{V} = \varepsilon_9\dot{\varepsilon}_9 + \varepsilon_{10}\dot{\varepsilon}_{10} \Rightarrow \Rightarrow \quad \varepsilon_9\dot{\varepsilon}_9 = \varepsilon_9(\dot{x}_9^d - x_{10}^d + \varepsilon_{10}) + \varepsilon_{10}(\dot{\varepsilon}_{10})$$

$$\varepsilon_{10}\left(\varepsilon_9 + \dot{x}_{10}^d + \frac{U_1}{m}U_y\right) = -K_{10}\varepsilon_{10}^2$$

Therefore:

$$U_y = \frac{m}{U_1}(-\varepsilon_9 - k_{10}\,\varepsilon_{10\_}k_9x_{10}) \tag{27}$$

2.3.6. Control x position
Underneath, (28) denotes the final sub-system:

$$\begin{cases} \dot{x}_{11} = x_{12} \\ \dot{x}_{12} = U_x\frac{U_1}{m} \end{cases} \tag{28}$$

Step 1

Defining ε_{11} the error between the actual position x and the desired one:

$$\varepsilon_{11} = x_{11}^d - x_{11} \Rightarrow \quad \dot{\varepsilon}_{11} = \dot{x}_{11}^d - \dot{x}_{11}$$

Lyapunov function is

$$V(\varepsilon_{11}) = \frac{1}{2}\varepsilon_{11}^2 \Rightarrow \dot{V}_{11} = \varepsilon_{11}\dot{\varepsilon}_{11}$$

Thus,

$$\dot{x}_{11}^d - x_{12} = -K_{11}\varepsilon_{11} \Rightarrow x_{12}^d = \dot{x}_{11}^d + K_{11}\varepsilon_{11}$$

Step 2

Set the error ε_{12} as:

$$\varepsilon_{12} = x_{12}^d - x_{12} \Rightarrow \dot{\varepsilon}_{12} = \dot{x}_{12}^d - \dot{x}_{12}$$

Thus,

$$V_{12} = V_{11} + \frac{1}{2}\varepsilon_{12}^2 \Rightarrow \dot{V}_{12} = \varepsilon_{11}\dot{\varepsilon}_{11} + \varepsilon_{12}\dot{\varepsilon}_{12}$$

Then

$$\varepsilon_{12}\left(\varepsilon_{11} + \dot{x}_{12}^d + \frac{U_1}{m}U_x\right) = -K_{12}\varepsilon_{12}^2$$

Therefore:

$$U_x = \frac{m}{U_1}(-\varepsilon_{11} - k_{12}\,\varepsilon_{12} - k_{11}x_{12}) \tag{29}$$

3. RESULTS AND DISCUSSION

MATLAB/Simulink is the most useful software used to test the behaviour of nonlinear systems and to validate the results of the recently developed controllers [38], [40], [41]. Therefore, model simulation is done using MATLAB/Simulink program to verify our suggested control approach. To achieve that, a quadrotor model is designed and controlled by three different controllers which are: PD, sliding mode and the BSC. Hence, each one of them is tested with and without disturbances to track a quadrotor's trajectory of radians R=8 shown in Figure 2. The chosen quadcopter's mass *m=200g*; whereas, the area moments of inertia *Ixx, Iyy* and *Izz* are 0.00025, 0.000232 and 0.0003738 respectively. The quadrotor has to track the trajectory defined by the time functions: $X = 8\sin(0.1t)$, $Y = 8\cos(0.1t)$ and $Z = 0.2t$.

3.1. Without disturbance

Figure 2(a) is an illustration of the trajectory tracked by the quadrotor. The next figures show the position, orientation (see Figures 2(b)-(d)), trajectory errors (illustrated in Figures 3(a)-(c)) and control inputs in the absence of disturbances generated by the three controllers: PDC (illustrated in Figure 4(a)), SMC (as shown in Figure 4(b)) and BSC (see Figure 4(c)) (see in appendix). Discussion: without any disturbance, the steady state error from the SMC was the smallest followed by PDC then the BSC for the displacement across both the X and Y axes. In the event that no disturbances, SMC has proven its efficiency even in the previous work [4], [20], [42]. However, for the displacement on the Z axis, the SMC did 10^{12} times worse than the BSC, with the PDC doing the best here. And finally, for the steady state error for yaw angle, the BSC also was 10^{17} better than the PDC, and the SMC and being lasting this category.

3.2. With disturbance

The next figures show the position and orientation (see Figures 5(a)-(c)) (see in appendix), the trajectory error Figures 6(a)-(c) (see in appendix) and control inputs (shown in Figures 7(a)-(c)) in the presence of a ramp disturbance of the vector F=9t i+9t j+ 9t k (N), starting from the 10th second of the simulation with a force limit of 9 N. Simulation are generated by applying the two controllers: PDC (shown Figure 5(a) and Figure 7(a)) and SMC (shown in Figure 5(b) and Figure 7(b)) versus BSC (illustrated in Figure 5(c) and

Figure 7(c)) (see in appendix). Discussion: now, in the case of disturbance. For small disturbance, the steady state error for every controller kept the same order as in case of no disturbance. But as the disturbance increased the controllers could not keep the quadrotor in trajectory anymore. The first controller that collapsed was the SMC. Making the PDC the best controller of the three under disturbance, but even this last one also collapsed after adding 133.33% of the first disturbance force. Then, BSC proves that it is the best to resist for all kind of disturbances; but, after adding about 50% of the previous disturbance force, the BSC collapsed too. However, the simulation result obtained from the implementation of the proposed BSC is very satisfactory compared to the previous works which show some complexity of the analytical inference and a considerable dynamic error, especially in presence of noise [4], [5], [43].
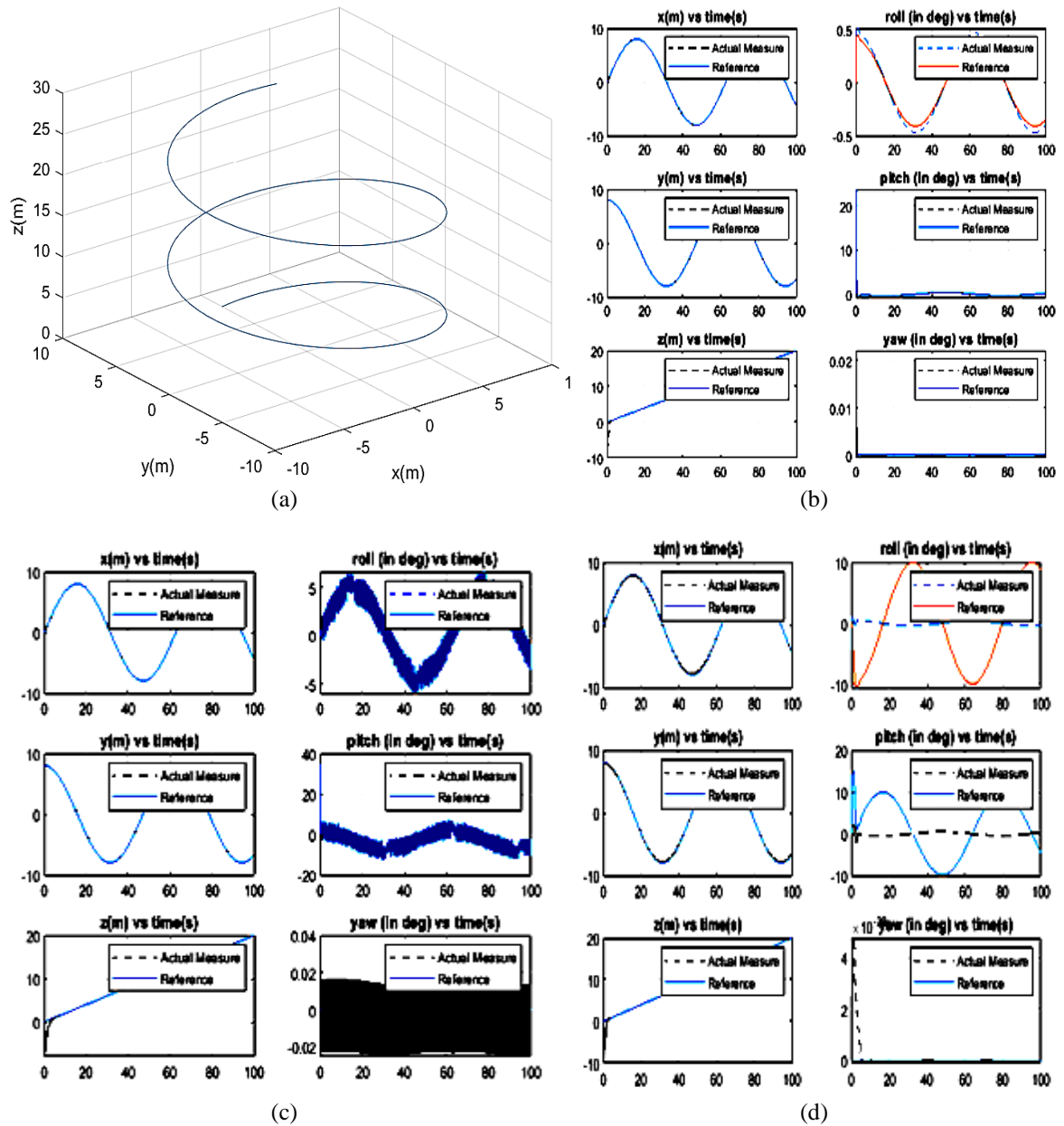
Figure 2. Attitude, heading and position reference (a) trajectory tracked by the quadrotor, (b) PDC, (c) SMC, and (d) BSC
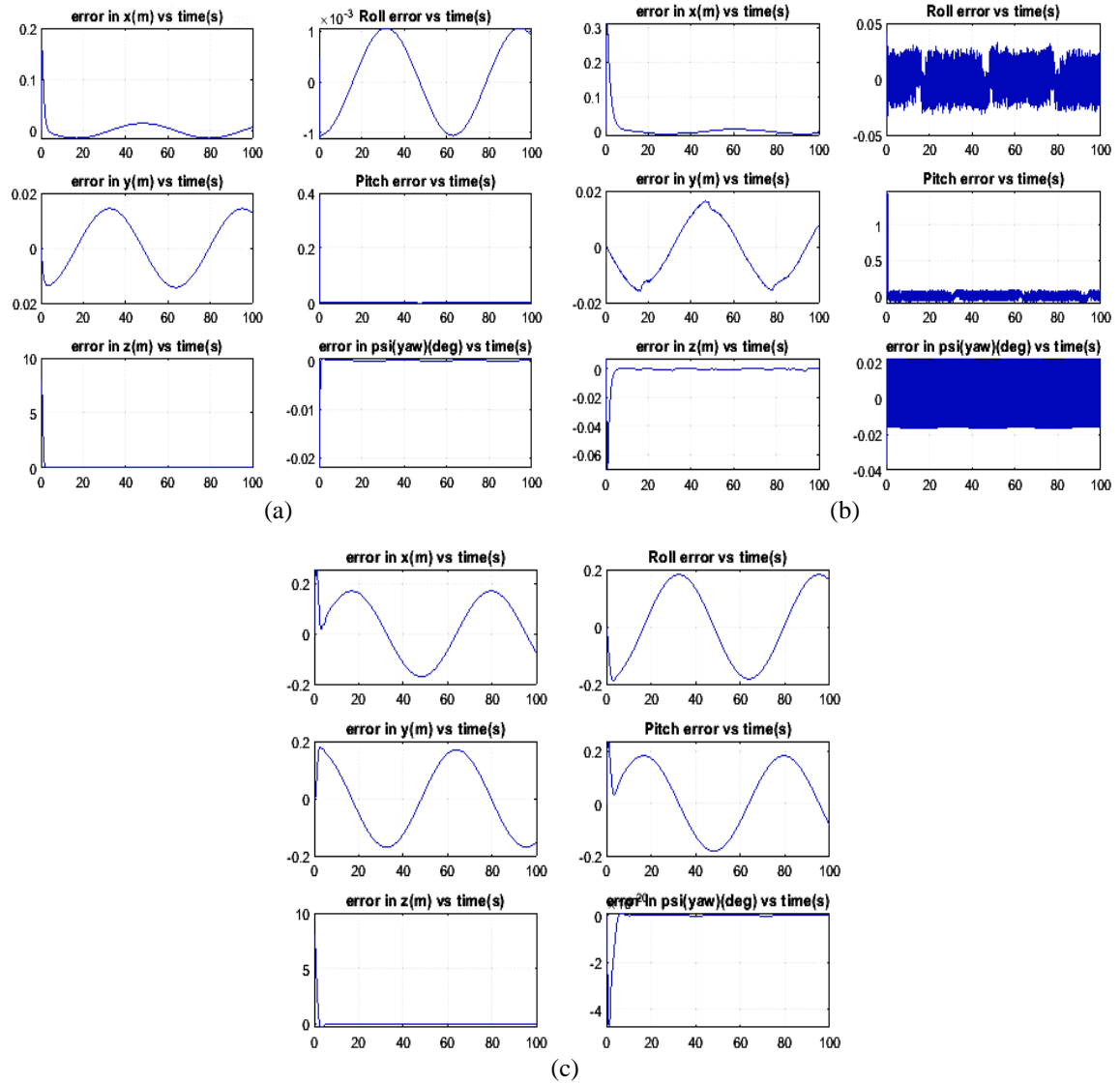
Figure 3. Altitude, heading, and position error signals (a) PDC, (b) SMC, and (c) BSC

4. CONCLUSION

This paper proposes a controller for quadrotor's trajectory tracking. First, kinematics and dynamics modeling of the quadrotor are developed which yield the motion's equations. Basing on this, an enhanced backstepping scheme is developed for position and orientation subsystems where stability analysis is ensured by Lyapunov concept.

It is established that the position, orientation and attitude path following errors can rapidly converge to slight values with all controllers. In case of non-external disturbance, BSC shows good control of the yaw angle and the altitude of the quadrotor comparing to the two other controllers (SMC and PDC). Moreover, in the case of presence of disturbances, for small disturbance, each controller's steady state error maintained the same order as in the absence of any disturbance. However, as the disturbance increase the controllers could not keep the quadrotor in trajectory anymore. Numerical and simulation results confirm that BSC is the last one that collapsed which confirm the robustness and efficacy of our constructed enhanced control strategy. Our perspectives involve improving the proposed approach; then, test and design it on real experimental quadrotor platform.

APPENDIX
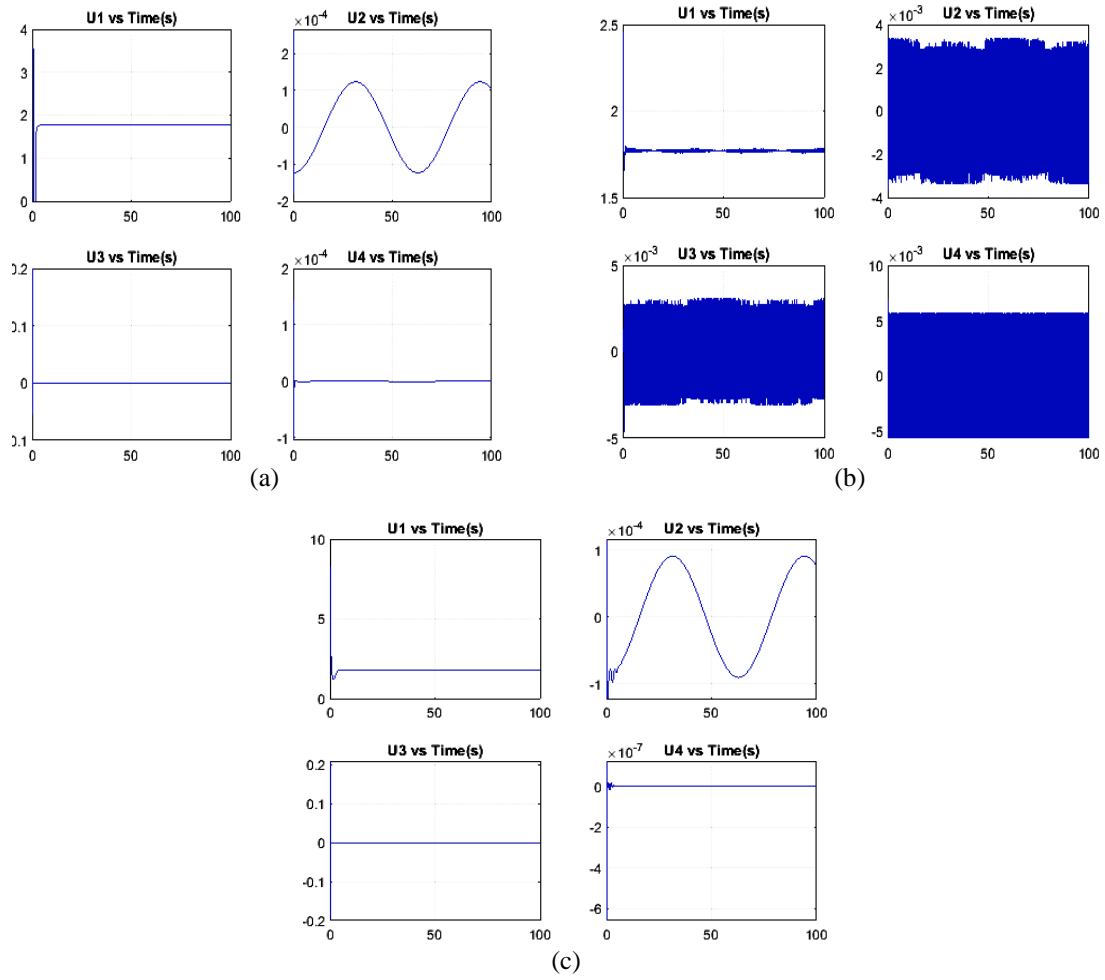
Figure 4. U1, U2, U3 and U4 vs. time, (a) PDC, (b) SMC, and (c) BSC
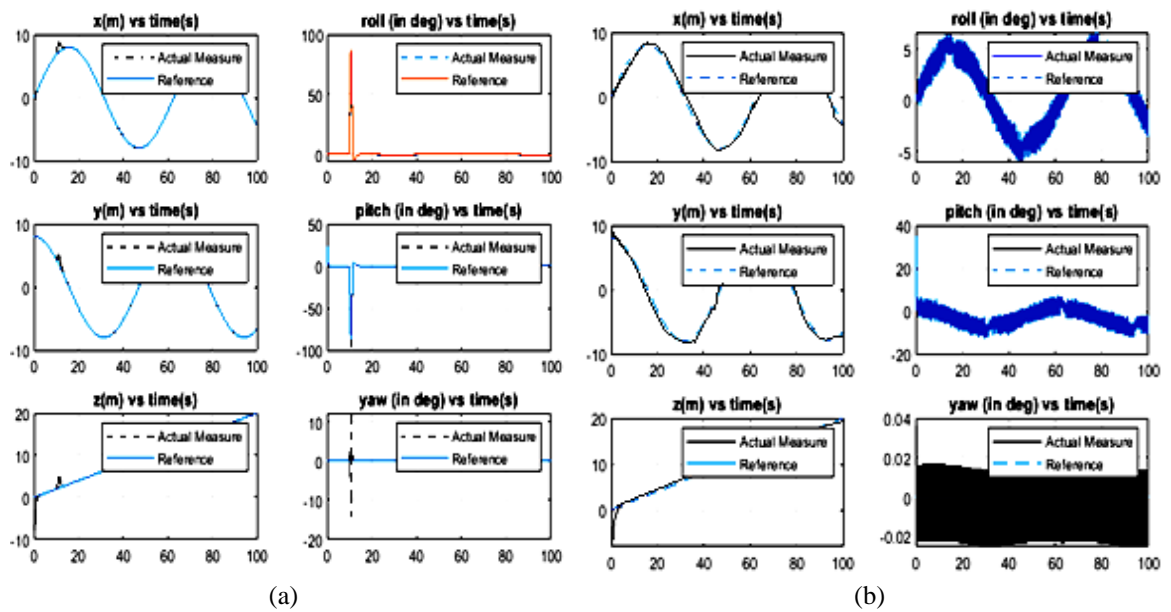
Figure 5. Altitude, heading and position reference measurement vs. actual measurement (a) PDC, (b) SMC

(c)

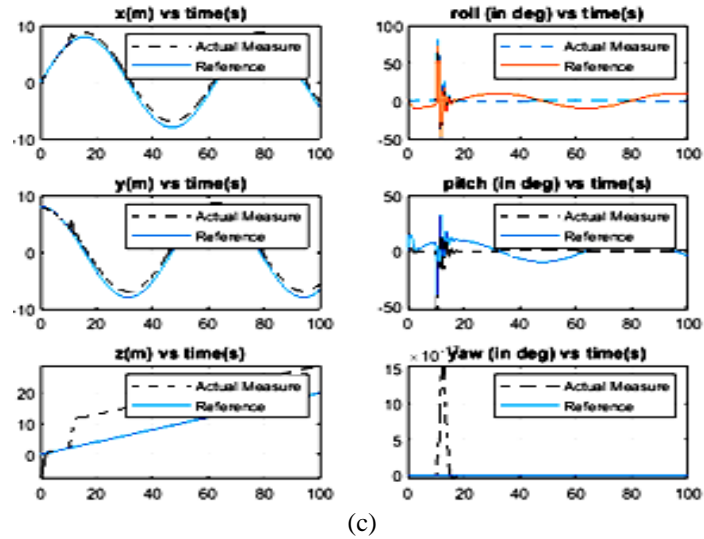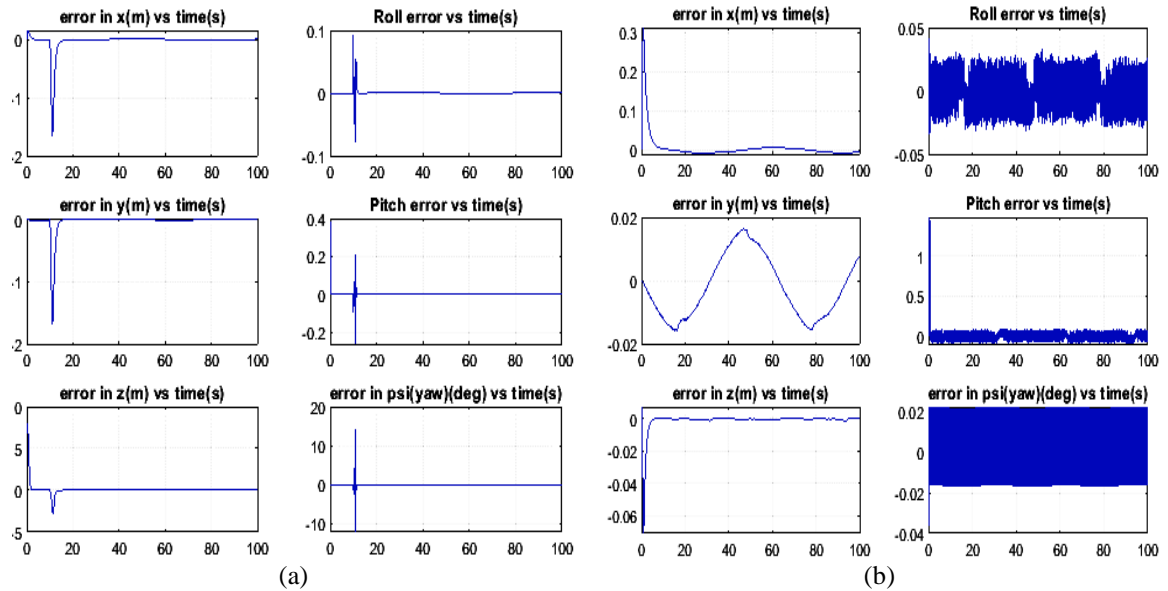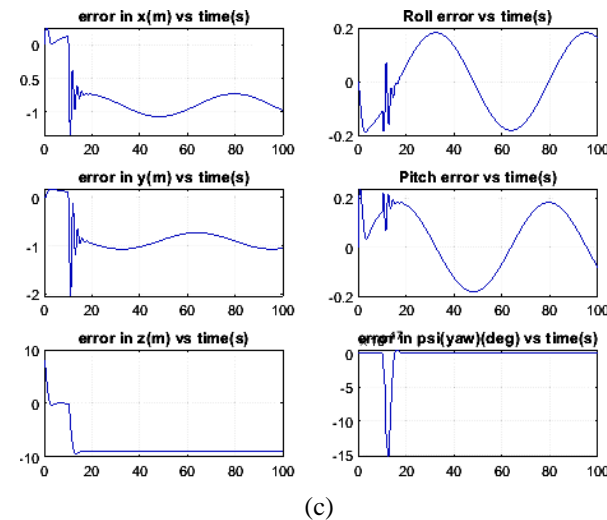Figure 5. Altitude, heading and position reference measurement vs. actual measurement (c) BSC (continue)

(a)   (b)

(c)

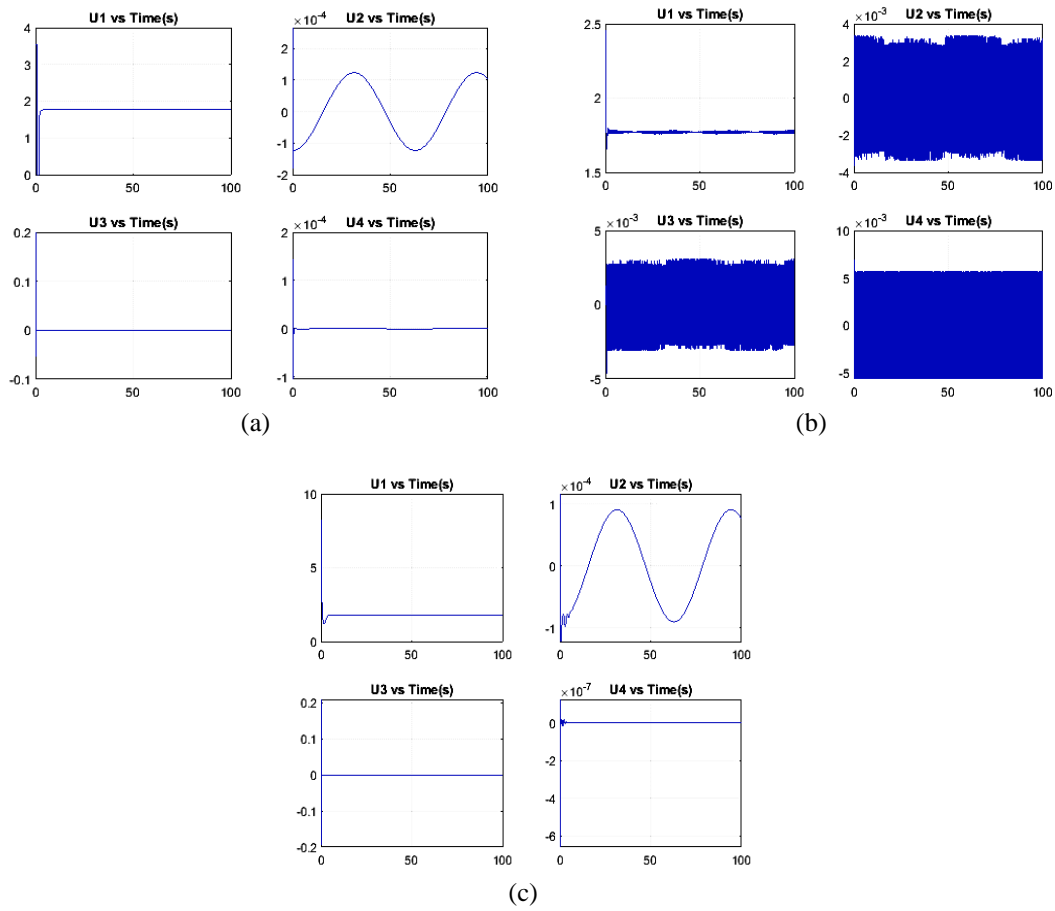Figure 6. Altitude, heading and position error signals (a) PDC, (b) SMC, and (c) BSC

(a)

(b)

(c)

Figure 7. U1, U2, U3, and U4 vs. time (a) PDC, (b) SMC, and (c) BSC

REFERENCES

[1] S. Agarwal, A. Mohan, and K. Kumar, "Design and fabrication of twinrotor UAV," in *Computer Science & Information Technology (CS & IT)*, Nov. 2013, pp. 369–377, doi: 10.5121/csit.2013.3830.

[2] H. Belaidi, H. Bentarzi, Z. Rabiai, and A. Abdelmoumene, "Multi-agent system for voltage regulation in smart grid," in *Artificial Intelligence and Renewables Towards an Energy Transition*, Springer International Publishing, 2021, pp. 487–499.

[3] H. Belaidi and Z. Rabiai, "Decentralized energy management system enhancement for smart grid," in *Research Anthology on Smart Grid and Microgrid Development*, IGI Global, 2022, pp. 77–90.

[4] L. -X. Xu, H. -J. Ma, D. Guo, A. -H. Xie, and D. -L. Song, "Backstepping sliding-mode and cascade active disturbance rejection control for a quadrotor UAV," *IEEE/ASME Transactions on Mechatronics*, vol. 25, no. 6, pp. 2743–2753, Dec. 2020, doi: 10.1109/TMECH.2020.2990582.

[5] M. A. Basri and A. Noordin, "Optimal backstepping control of quadrotor UAV using gravitational search optimization algorithm," *Bulletin of Electrical Engineering and Informatics*, vol. 9, no. 5, pp. 1819–1826, Oct. 2020, doi: 10.11591/eei.v9i5.2159.

[6] H. J. Zhu, X. G. Meng, and M. Sun, "Forward flight stability in a drone-fly," *Scientific Reports*, vol. 10, no. 1, pp. 1-12, Dec. 2020, doi: 10.1038/s41598-020-58762-5.

[7] P. Govindan, "Evolutionary algorithms based tuning of PID controller for an AVR system," *International Journal of Electrical and Computer Engineering (IJECE)*, vol. 10, no. 3, pp. 3047-3056, Jun. 2020, doi: 10.11591/ijece.v10i3.pp3047-3056.

[8] M. M. A. Alqadasi, S. M. Othman, M. F. Rahmat, and F. Abdullah, "Optimization of PID for industrial electro-hydraulic actuator using PSOGSA," *TELKOMNIKA (Telecommunication Computing Electronics and Control)*, vol. 17, no. 5, pp. 2625-2635, Oct. 2019, doi: 10.12928/telkomnika.v17i5.12808.

[9] W. Aribowo, S. Supari, and B. Suprianto, "Optimization of PID parameters for controlling DC motor based on the aquila optimizer algorithm," *International Journal of Power Electronics and Drive Systems (IJPEDS)*, vol. 13, no. 1, pp. 216-222, Mar. 2022, doi: 10.11591/ijpeds.v13.i1.pp216-222.

[10] Q.-V. Ngo, C. Yi, and T. -T. Nguyen, "The fuzzy-PID based-pitch angle controller for small-scale wind turbine," *International Journal of Power Electronics and Drive Systems (IJPEDS)*, vol. 11, no. 1, pp. 135-142, Mar. 2020, doi: 10.11591/ijpeds.v11.i1.pp135-142.

[11] R. S. Raheem, M. Y. Hassan, and S. K. Kdahim, "Particle swarm optimization based interval type 2 fuzzy logic control for motor rotor position control of artificial heart pump," *Indonesian Journal of Electrical Engineering and Computer Science*, vol. 25, no. 2, pp. 814-824, Feb. 2022, doi: 10.11591/ijeecs.v25.i2.pp814-824.

[12] W. R. A. -Adheem, "Design and simulation of a normalized fuzzy logic controller for the quadruple-tank process," *Indonesian Journal of Electrical Engineering and Computer Science*, vol. 18, no. 1, pp. 227-234, Apr. 2020, doi: 10.11591/ijeecs.v18.i1.pp227-234.

[13] F. N. Zohedi, M. S. M. Aras, H. A. Kasdirin, and N. B. Nordin, "New lambda tuning approach of single input fuzzy logic using gradient descent algorithm and particle swarm optimization," *Indonesian Journal of Electrical Engineering and Computer Science*,

vol. 25, no. 3, pp. 1344-1355, Mar. 2022, doi: 10.11591/ijeecs.v25.i3.pp1344-1355.

[14] N. M. Ameen and A. T. Humod, "Robust nonlinear PD controller for ship steering autopilot system based on particle swarm optimization technique," *IAES International Journal of Artificial Intelligence (IJ-AI)*, vol. 9, no. 4, pp. 662-669, Dec. 2020, doi: 10.11591/ijai.v9.i4.pp662-669.

[15] M. A. Faraj and A. M. Abbood, "Fractional order PID controller tuned by bat algorithm for robot trajectory control," *Indonesian Journal of Electrical Engineering and Computer Science*, vol. 21, no. 1, pp. 74-83, Jan. 2021, doi: 10.11591/ijeecs.v21.i1.pp74-83.

[16] A. Houari, I. Bachir, D. K. Mohame, and M. K. Mohamed, "PID vs LQR controller for tilt rotor airplane," *International Journal of Electrical and Computer Engineering (IJECE)*, vol. 10, no. 6, p. 6309-6318, Dec. 2020, doi: 10.11591/ijece.v10i6.pp6309-6318.

[17] L. Ardhenta and T. Nurwati, "Comparison of sliding mode controller application for buck-boost converter based on linear sliding surface," *International Journal of Power Electronics and Drive Systems (IJPEDS)*, vol. 13, no. 1, pp. 423-431, Mar. 2022, doi: 10.11591/ijpeds.v13.i1.pp423-431.

[18] M. Labbadi, M. Cherkaoui, Y. E. Houm, and M. Guisser, "Modeling and robust integral sliding mode control for a quadrotor unmanned aerial vehicle," in *2018 6th International Renewable and Sustainable Energy Conference (IRSEC)*, Dec. 2018, pp. 1–6, doi: 10.1109/IRSEC.2018.8702881.

[19] S. Zahran, A. Moussa, and N. E. -Sheimy, "Enhanced drone navigation in GNSS denied environment using VDM and hall effect sensor," *ISPRS International Journal of Geo-Information*, vol. 8, no. 4, pp. 1-18, Apr. 2019, doi: 10.3390/ijgi8040169.

[20] T. D. Chuyen, V. H. Nguyen, P. N. Dao, N. A. Tuan, and N. Van Toan, "Sliding mode control strategy based lead screw control design in electromechanical tracking drive system," *International Journal of Power Electronics and Drive Systems (IJPEDS)*, vol. 13, no. 1, pp. 150-158, Mar. 2022, doi: 10.11591/ijpeds.v13.i1.pp150-158.

[21] A. Noordin, M. A. M. Basri, Z. Mohamed, and I. M. Lazim, "Adaptive PID controller using sliding mode control approaches for quadrotor UAV attitude and position stabilization," *Arabian Journal for Science and Engineering*, vol. 46, no. 2, pp. 963–981, Feb. 2021, doi: 10.1007/s13369-020-04742-w.

[22] A. A. Najm and I. K. Ibraheem, "Nonlinear PID controller design for a 6-DOF UAV quadrotor system," *Engineering Science and Technology, an International Journal*, vol. 22, no. 4, pp. 1087–1097, Aug. 2019, doi: 10.1016/j.jestch.2019.02.005.

[23] R. Thusoo, S. Jain, and S. Bangia, "PID control of a quadrotor," in *Advances in Communication and Computational Technology*, 2021, pp. 633–645.

[24] B. Tian, J. Cui, H. Lu, Z. Zuo, and Q. Zong, "Adaptive finite-time attitude tracking of quadrotors with experiments and comparisons," *IEEE Transactions on Industrial Electronics*, vol. 66, no. 12, pp. 9428–9438, Dec. 2019, doi: 10.1109/TIE.2019.2892698.

[25] F. Chen, Q. Wu, B. Jiang, and G. Tao, "A reconfiguration scheme for quadrotor helicopter via simple adaptive control and quantum logic," *IEEE Transactions on Industrial Electronics*, vol. 62, no. 7, pp. 4328–4335, Jul. 2015, doi: 10.1109/TIE.2015.2389760.

[26] A. Tzes, G. Nikolakopoulos, and K. Alexis, "Model predictive quadrotor control: attitude, altitude and position experimental studies," *IET Control Theory & Applications*, vol. 6, no. 12, pp. 1812–1827, Aug. 2012, doi: 10.1049/iet-cta.2011.0348.

[27] D. T. Nguyen, N. P. Dao, and H. T. T. Lai, "Modelling and control design of the electrostatic linear comb actuator," *International Journal of Power Electronics and Drive Systems (IJPEDS)*, vol. 13, no. 2, pp. 805-811, Jun. 2022, doi: 10.11591/ijpeds.v13.i2.pp805-811.

[28] E. A. Chater, H. Housny, and H. E. Fadil, "Adaptive proportional integral derivative deep feedforward network for quadrotor trajectory-tracking flight control," *International Journal of Electrical and Computer Engineering (IJECE)*, vol. 12, no. 4, p. 3607-3619, Aug. 2022, doi: 10.11591/ijece.v12i4.pp3607-3619.

[29] V. T. Ha, L. T. Tan, N. D. Nam, and N. P. Quang, "Backstepping control of two-mass system using induction motor drive fed by voltage source inverter with ideal control performance of stator current," *International Journal of Power Electronics and Drive Systems (IJPEDS)*, vol. 10, no. 2, pp. 720-730, Jun. 2019, doi: 10.11591/ijpeds.v10.i2.pp720-730.

[30] R. Majdoul, A. Touati, A. Ouchatti, A. Taouni, and E. Abdelmounim, "Comparison of backstepping, sliding mode and PID regulators for a voltage inverter," *International Journal of Electrical and Computer Engineering (IJECE)*, vol. 12, no. 1, pp. 166-178, Feb. 2022, doi: 10.11591/ijece.v12i1.pp166-178.

[31] P. E. I. Pounds, "Design, construction and control of a large quadrotor micro air vehicle," Australian National University, 2007.

[32] Fahmizal, A. Surriani, M. Budiyanto, and M. Arrofiq, "Altitude control of quadrotor using fuzzy self tuning PID controller," in *2017 5th International Conference on Instrumentation, Control, and Automation (ICA)*, Aug. 2017, pp. 67–72, doi: 10.1109/ICA.2017.8068415.

[33] N. Nagui, O. Attallah, M. S. Zaghloul, and I. Morsi, "Improved GPS/IMU loosely coupled integration scheme using two kalman filter-based cascaded stages," *Arabian Journal for Science and Engineering*, vol. 46, no. 2, pp. 1345–1367, Feb. 2021, doi: 10.1007/s13369-020-05144-8.

[34] N. V. Tan, K. N. Dang, P. D. Dai, and L. V. Van, "Position control for haptic device based on discrete-time proportional integral derivative controller," *International Journal of Electrical and Computer Engineering (IJECE)*, vol. 12, no. 1, pp. 269-279, Feb. 2022, doi: 10.11591/ijece.v12i1.pp269-276.

[35] S. Bouabdallah, A. Noth, and R. Siegwart, "PID vs LQ control techniques applied to an indoor micro quadrotor," in *2004 IEEE/RSJ International Conference on Intelligent Robots and Systems (IROS) (IEEE Cat. No.04CH37566)*, vol. 3, pp. 2451–2456, doi: 10.1109/IROS.2004.1389776.

[36] V. Mistler, A. Benallegue, and N. K. M'Sirdi, "Exact linearization and noninteracting control of a 4 rotors helicopter via dynamic feedback," in *Proceedings 10th IEEE International Workshop on Robot and Human Interactive Communication. ROMAN 2001 (Cat. No.01TH8591)*, pp. 586–593, doi: 10.1109/ROMAN.2001.981968.

[37] A. Saibi, R. Boushaki, and H. Belaidi, "Backstepping control of drone," in *ICCEIS 2021*, Jan. 2022, pp. 1-9, doi: 10.3390/engproc2022014004.

[38] H. B. Lai, A.-T. Tran, V. Huynh, E. N. Amaefule, P. T. Tran, and V.-D. Phan, "Optimal linear quadratic Gaussian control based frequency regulation with communication delays in power system," *International Journal of Electrical and Computer Engineering (IJECE)*, vol. 12, no. 1, pp. 157-165, Feb. 2022, doi: 10.11591/ijece.v12i1.pp157-165.

[39] D. H. Phan, M. T. Dao, V. T. Nguyen, H. A. Bui, N. D. Le, and T. L. Bui, "Design of super-twisting algorithm control and observer for three-phase inverter in standalone operation," *International Journal of Power Electronics and Drive Systems (IJPEDS)*, vol. 13, no. 1, pp. 368-379, Mar. 2022, doi: 10.11591/ijpeds.v13.i1.pp368-379.

[40] N. H. Abbas, "Tuning of different controlling techniques for magnetic suspending system using an improved bat algorithm," *International Journal of Electrical and Computer Engineering (IJECE)*, vol. 10, no. 3, pp. 2402-2415, Jun. 2020, doi: 10.11591/ijece.v10i3.pp2402-2415.

[41] A. Abdalhadi, H. Wahid, and D. H. Burhanuddin, "An optimal proportional integral derivative tuning for a magnetic levitation system using metamodeling approach," *Indonesian Journal of Electrical Engineering and Computer Science*, vol. 25, no. 3, pp. 1356-1366, Mar. 2022, doi: 10.11591/ijeecs.v25.i3.pp1356-1366.

[42] H. Nurhadi, E. Apriliani, T. Herlambang, and D. Adzkiya, "Sliding mode control design for autonomous surface vehicle motion under the influence of environmental factor," *International Journal of Electrical and Computer Engineering (IJECE)*, vol. 10, no. 5, pp. 4789-4797, Oct. 2020, doi: 10.11591/ijece.v10i5.pp4789-4797.

[43] D. Kucherov, A. Kozub, O. Sushchenko, and R. Skrynkovskyy, "Stabilizing the spatial position of a quadrotor by the backstepping procedure," *Indonesian Journal of Electrical Engineering and Computer Science*, vol. 23, no. 2, pp. 1188-1199, Aug. 2021, doi: 10.11591/ijeecs.v23.i2.pp1188-1199.

BIOGRAPHIES OF AUTHORS

Ali Saibi was born in Zmalet Emir Abdelkader, Algeria, in 1967. He received engineer degree in Electrical Engineering from the University of Ibn. Khaldoun, Tiaret in 1993. He was appointed as an engineer professor at Department Electrical of Ibn. Khaldoun University in 1993. He received his M.S degree in control engineering from polytechnic school of Algiers, Algeria in 2006. Currently, he is preparing his Ph.D. in Electrical Engineering Institute of Electrical and Electronic Engineering, University M'hamed Bougara of Boumerdes since 2019. His research interests are control of systems and electrical systems. He can be contacted at email: alisaibimag@yahoo.fr and a.saibi@univ-boumerdes.dz.

Hadjira Belaidi received her Doctorate degree from Institute of Electrical and Electronic Engineering, University M'hamed Bougara of Boumerdes in 2015. She has been an assistant professor at Institute of Electrical and Electronic Engineering since 2014. Currently, she is the leader of ''Embedded Systems and Robotics'' team in the Signals and Systems Laboratory, as well as a lecturer at Department of Electronic at Institute of Electrical and Electronic Engineering, University M'hamed Bougara of Boumerdes, Algeria. Her research interests include all-terrain mobile robots, environment modeling and manipulator robots, drones control, and smart-grid. She can be contacted at email: ha.belaidi@univ-boumerdes.dz.

Razika Boushaki is a Teacher in Electrical Engineering at the university of Boumerdes (Algeria) in the Institute of Electrical and Electronic Engineering since 2003. She obtained Engineer Diploma in 1995, magister Diploma in 2003 at University of Boumerdes and Doctorate degree in June 2013, in Electrical Engineering. She is member in the research laboratory since 2009. She introduced several practical automation systems in industry between 1999 and 2003. Currently, she is Prof. at Institute of Electrical and Electronic Engineering, University M'hamed Bougara of Boumerdes, Algeria. Her research interests include intelligent control, fuzzy logic control, advanced control, nonlinear control and adaptive control. She can be contacted at email: boushakiraz@yahoo.fr and r.boushaki@univ-boumerdes.dz.

Recham Zine Eddine He was a Master student in Automatic "Control" at Institute of Electrical and Electronic Engineering at University M'hamed Bougara of Boumerdes, Algeria in september 2021. He got his Bachelor degree in Electrical and Electronics Engineering from the same institute which was achieved in June 2019. His bachelor degree project was entitled "Free space data acquisition system and reading the data on a smartphone using gyroscope sensor and arduino". Whereas, his master project was entitled: "Adaptive control for disturbance rejection in quadrotors" released on September 2021. He can be contacted at email: recham.zineeddine99@gmail.com.

Amrouche Hafid He got his Bachelor degree in Electrical and Electronics Engineering from the University M'hamed Bougara of Boumerdes, Algeria in June 2019. Then, received his Master degree in Automatic "Control" from the same Institute in September 2021. His final master project was entitled: "Adaptive control for disturbance rejection in quadrotors" reaslised on september 2021. He can be contacted at email: hafidamrouche8@gmail.com.